

Contribution from the Istituto per lo Studio della Stereochimica ed Energetica dei Composti di Coordinazione del CNR, Via J. Nardi 39, 50132, Firenze, Italy

Classical and Nonclassical Polyhydride Ruthenium(II) Complexes Stabilized by the Tetrphosphine $P(CH_2CH_2PPh_2)_3$

Claudio Bianchini,* Pedro J. Perez,[†] Maurizio Peruzzini, Fabrizio Zanobini, and Alberto Vacca

Received June 5, 1990

The dichloride $[(PP_3)RuCl_2]$ (**1**) is selectively transformed into $[(PP_3)Ru(H)(\eta^1-BH_4)]$ (**2**), $[(PP_3)Ru(H)Cl]$ (**3**), and $[(PP_3)Ru(H)_2]$ (**4**) by reaction with $NaBH_4$, $LiHBEt_3$, and $LiAlH_4$, respectively [$PP_3 = P(CH_2CH_2PPh_2)_3$]. Complex **2** is fluxional on the NMR time scale in ambient-temperature solutions due to equilibration of the BH_4^- hydrogens through cleavage of the Ru–H₅–B bridge and interconversion of H₁ by rotation. The hydride–tetrahydroborate complex exhibits amphoteric nature: it reacts with protic acids, yielding the *cis*-hydride–dihydrogen complex $[(PP_3)Ru(H)(\eta^2-H_2)]Y$ ($Y = PF_6$, **6a**; BPh_4 , **6b**), and with bases such as PEt_3 or KO^tBu , converting to the dihydride **4**. The latter compound can be obtained also by thermal decomposition of **2** in refluxing toluene or benzene. Complexes **6a,b** can be prepared by reaction of the dihydride **4** with protic acids. The nonclassical structure of **6a,b** is established by variable-temperature 1H and ^{31}P NMR data, T_1 measurements and $J(HD)$ values. In the solid state and in solution at low temperature $[(PP_3)Ru(H)(\eta^2-H_2)]^+$ is octahedral, and the hydride and dihydrogen ligands occupy mutually *cis* positions. At ambient temperature in solution the complex is trigonal-bipyramidal and the equilibration of the hydrogens might proceed through an "H₃" unit occupying an axial position trans to the bridgehead phosphorus atom of PP_3 . Octahedral monohydride complexes of the type $[(PP_3)Ru(H)(L)]BPh_4$ are obtained from **6b** by substitution of dihydrogen with the appropriate ligand ($L = N_2, CO, PEt_3, CH_3CN, SO_2$). In all cases, the hydride ligand is located trans to a terminal phosphorus of the ligand. The role played by the tripodal tetradentate phosphine PP_3 in the stabilization, in the fluxionality, and in the structure of all of the present Ru complexes is amply discussed.

Introduction

Group VIII metal complexes with the potentially tetradentate phosphine $P(CH_2CH_2PPh_2)_3$ (PP_3) are attracting considerable interest in homogeneous catalysis, particularly for those reactions that do not require too many open sites at the metal.¹ In actuality, the chelating nature of PP_3 may prevent M–P bond dissociation, thus limiting the number of free coordination sites along the reaction pathway. This unfavorable feature of PP_3 , and, in general, of polyphosphine ligands, can be overcome by inserting into the metal coordination sphere one or two coligands exhibiting either strong trans influence, such as hydride, or weak coordinating capability, such as dihydrogen. As a matter of fact, the monohydrides $[(PP_3)CoH]$ ^{1a} and $[(PP_3)RhH]$ ^{1b} prove good catalysts for linear and cyclic oligomerization reactions of alkynes, while the η^2-H_2 complexes $[(PP_3)Rh(H_2)]^+$ ^{1c} and $[(PP_3)Co(H_2)]^+$ ^{1d} are catalyst precursors for the synthesis of enol esters from 1-alkynes and carboxylic acids and for *cis* → *trans* isomerization reactions of disubstituted alkenes, respectively.

The combination of hydride and dihydrogen ligands at $(PP_3)M$ fragments seems to be particularly rich in chemical implications, as shown by the participation of $[(PP_3)FeH(H_2)]^+$ in a wide range of stoichiometric and catalytic reactions, including the selective hydrogenation of 1-alkynes to alkenes and the reductive dimerization of 1-alkynes to 1,4-disubstituted butadienes.^{1e}

Attracted by ruthenium, which is considered *the metal of the future in homogeneous catalysis*² for its ability to coordinate several participative ligands and readily enter into the 0 = II = IV oxidation/reduction cycle, we initiated a systematic study of the coordination chemistry involving PP_3 and ruthenium(II).

In this paper, we describe the synthesis and characterization of several novel ruthenium(II) PP_3 complexes containing hydride and/or dihydrogen ligands. Of particular relevance is the complex $[(PP_3)Ru(H)(\eta^2-H_2)]^+$, where hydride and dihydrogen are forced mutually *cis* by the tripodal structure of the polyphosphine ligand. Such an unusual arrangement for hydride and dihydrogen ligands provides the complex with interesting chemical–physical properties.

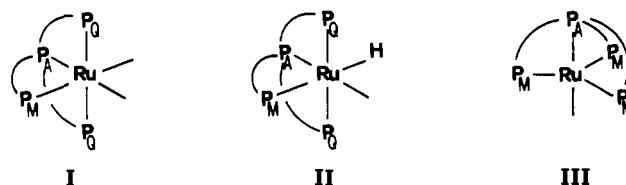
Results

Synthesis and Characterization of the Complexes. The preparations and principal reactions of the complexes described in this

paper are summarized in Scheme I. Selected NMR spectral data are collected in Table I ($^{31}P\{^1H\}$ NMR spectra) and Table II (1H NMR spectra). The latter includes also significant IR absorptions.

$[(PP_3)RuCl_2]$. The dichloride $[(PP_3)RuCl_2]$ (**1**) constitutes an excellent entry to mono- and polyhydride ruthenium(II) complexes stabilized by the tripodal tetradentate ligand PP_3 . Compound **1** is synthesized in good yield (>85%) by reaction of $[RuCl_2(DMSO)_4]$ ($DMSO = \text{dimethyl sulfoxide}$) with an equivalent amount of PP_3 in refluxing toluene for 2 h. Longer times or less vigorous reaction conditions lower the yield. Alternatively, **1** can be obtained in ca. 75% yield by reacting $[RuCl_2(PPh_3)_4]$ with PP_3 in refluxing toluene. Despite the lower yield, this second route may be preferable due to the absence of malodorous byproducts originating from decomposition of DMSO during the synthesis of $[RuCl_2(DMSO)_4]$.

Compound **1** is a pale yellow crystalline material that crystallizes as the dichloromethane solvate in analytically pure form from dichloromethane/ethanol mixtures. It is stable in the solid state and in deoxygenated solutions, where it behaves as a nonelectrolyte. The $^{31}P\{^1H\}$ NMR spectrum in $CDCl_3$ consists of a simple first-order AMQ_2 splitting pattern, which is typical for all of the octahedral (OCT) Ru complexes herein described (I).

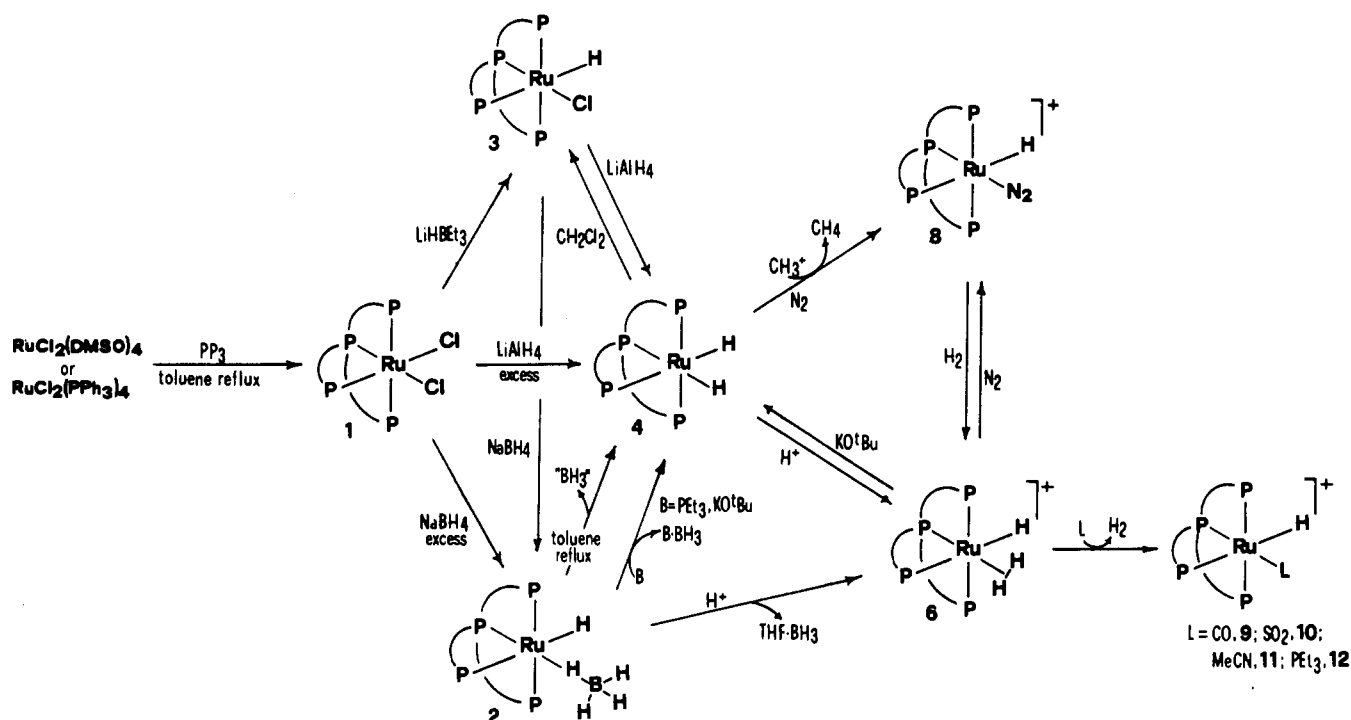


The spectrum shows three well-separated resonances of relative intensities 1:1:2 (AMQ_2 splitting pattern) and is temperature-invariant down to $-100^\circ C$. The highest frequency resonance (δ

- (1) (a) Bianchini, C.; Innocenti, P.; Meli, A.; Peruzzini, M.; Zanobini, F.; Zanello, P. *Organometallics* 1990, 9, 2514. (b) Bianchini, C.; Meli, A.; Peruzzini, M.; Vizza, F.; Frediani, P. *Organometallics* 1990, 9, 1146. (c) Bianchini, C.; Meli, A.; Peruzzini, M.; Zanobini, F.; Bruneau, C.; Dixneuf, P. *Organometallics* 1990, 9, 1155. (d) Bianchini, C.; Mealli, C.; Meli, A.; Peruzzini, M.; Zanobini, F. *J. Am. Chem. Soc.* 1988, 110, 8725. (e) Bianchini, C.; Meli, A.; Peruzzini, M.; Vizza, F.; Zanobini, F.; Frediani, P. *Organometallics* 1989, 8, 2080.
- (2) James, B. R. Paper presented at the Symposium on New Science in Homogeneous Transition Metal Catalyzed Reactions, 199th National Meeting of the American Chemical Society, Boston, MA, April 22–27, 1990.

[†] Permanent address: Departamento de Quimica Inorganica, Facultad de Quimica, Universidad de Sevilla, Sevilla, Spain.

Scheme I

Table I. $^{31}\text{P}\{^1\text{H}\}$ NMR Data for the Complexes^a

compd	solvent	temp, K	pattern	chem shift, ppm ^b			coupling const <i>J</i> , Hz		
				$\delta(\text{P}_A)$	$\delta(\text{P}_M)$	$\delta(\text{P}_Q)$	P_AP_M	P_AP_Q	P_MP_Q
1	CHCl_3	293	AMQ_2	153.64	65.70	40.40	14.7	8.0	24.5
2	CH_2Cl_2	293	AMQ_2	150.84	39.58	50.01	6.7	14.2	2.0
3	CH_2Cl_2	293	AMQ_2	152.29	54.00	60.42	9.1	13.6	14.2
4	C_7H_8	305	AM_3	157.30	77.84		7.7		
6	$\text{CH}_3\text{COCH}_3^d$	198	AMQ_2	156.58	75.73	79.55	<i>c</i>	<i>c</i>	<i>c</i>
		203	AMQ_2	147.70	66.51	69.23	12.4	12.4	13.0
8	CH_3COCH_3	293	AMQ_2	150.87	44.13	59.75	2.0	12.7	13.4
9	CH_3COCH_3	293	AMQ_2	142.68	62.17	64.65	14.9	14.9	14.9
10	CH_3NO_2	293	AMQ_2	140.67	64.20	57.83	9.7	16.0	12.6
11	CH_2Cl_2	293	AMQ_2	147.13	59.12	47.31	6.8	12.9	12.9
12	CH_2Cl_2	293	AMQ_2V^e	146.67	59.15	61.30	7.0	18.0	12.3

^aAt 121.42 MHz. ^bChemical shift values (δ 's) are relative to 85% H_3PO_4 with positive values being downfield from the standard. P_A refers to the bridgehead phosphorus atom of the PP_3 ligand, whereas P_M and P_Q denote the terminal phosphorus atoms. ^cBroad resonances. ^dThe spectrum was recorded under an atmosphere of dihydrogen. ^e P_V refers to the triethylphosphine ligand; $\delta = 6.05$ ppm; $J(\text{P}_A\text{P}_V) = 211.5$, $J(\text{P}_M\text{P}_V) = 28.9$, $J(\text{P}_Q\text{P}_V) = 28.3$ Hz.

= 153.64 ppm) can be readily attributed to the bridgehead phosphorus atom of the PP_3 ligand.^{1,3} This resonance appears as a doublet of triplets and originates from coupling to the phosphorus atom P_M trans to one of the two chloride ligands and from coupling to the two equivalent terminal phosphorus P_Q located in the axial positions of the octahedron. The resonance for the two mutually trans phosphorus atoms, P_Q , at δ 40.40 ppm, consists of a doublet of doublets and is due to coupling to the residual terminal phosphorus atom, P_M , and to the apical phosphorus atom, P_A . Finally, the remaining resonance, which appears as a triplet of doublets at δ 65.70 ppm, is ascribable to the terminal P_M atom. This multiplicity arises from coupling to the two equivalent P_Q atoms and to the bridgehead donor P_A . The splitting

pattern, chemical shifts, and coupling constants observed for **1** are consistent with an OCT geometry around ruthenium (II) where two chloride ligands are forced cis by the tripodal geometry of PP_3 .³

Reaction of 1 with NaBH_4 . Synthesis of $[(\text{PP}_3)\text{Ru}(\text{H})(\eta^1\text{-BH}_4)]$ (2). Pale cream-colored crystals of the hydride-tetrahydroborate complex $[(\text{PP}_3)\text{Ru}(\text{H})(\eta^1\text{-BH}_4)]$ (**2**) are quantitatively obtained by stirring **1** in THF for 1 h with a 2-fold excess of NaBH_4 dissolved in ethanol at 50 °C. Compound **2** is the only product of the reaction between **1** and NaBH_4 , even when a large excess of the latter reagent is used. For a stoichiometric amount of NaBH_4 , the formation of the *cis*-hydride-chloride complex $[(\text{P-P}_3)\text{Ru}(\text{H})\text{Cl}]$ (**3**) (see below) prevails over formation of **2**.

Complex **2** is stable in the solid state and in deoxygenated solutions, where it behaves as a nonelectrolyte. The IR spectrum exhibits a set of highly diagnostic bands in the 2360–1985- cm^{-1} region, where the stretching vibrations of the Ru–H–B, Ru–H, and B–H bonds are expected to fall.⁴ In particular, two strong absorptions at 2360 and 2270 cm^{-1} are assigned to the terminal

(3) For example: (a) Bianchini, C.; Masi, D.; Meli, A.; Peruzzini, M.; Zanolini, F. *J. Am. Chem. Soc.* **1988**, *110*, 6411. (b) Bianchini, C.; Meli, A.; Peruzzini, M.; Ramirez, J. A.; Vacca, A.; Vizza, F.; Zanolini, F. *Organometallics* **1989**, *8*, 337. (c) Bianchini, C.; Masi, D.; Meli, A.; Peruzzini, M.; Ramirez, J. A.; Vacca, A.; Zanolini, F. *Organometallics* **1989**, *8*, 2179. (d) DuBois, D. L.; Miedaner, A. *Inorg. Chem.* **1986**, *25*, 4642. (e) Gambaro, J. J.; Hohman, W. H.; Meek, D. W. *Inorg. Chem.* **1989**, *28*, 4154. (f) Antberg, M.; Dahlenburg, L.; Frosin, K. M.; Höcke, N. *Chem. Ber.* **1988**, *121*, 859.

(4) (a) Marks, T. J.; Kolb, J. R. *Chem. Rev.* **1977**, *77*, 263. (b) Teller, R. G.; Bau, R. *Struct. Bonding (Berlin)* **1981**, *44*, 3.

Table II. Selected IR and ^1H NMR Spectral Data for the Complexes^a

compd	solvnt	temp, K	δ , ppm	multiplicity ^b	assgnt (intensity)	coupling constant		$\nu(\text{Ru-H})$, ^d cm^{-1}	other abs, ^d cm^{-1}				
						value, Hz	type ^c						
2	CD_2Cl_2	293	-8.52	dtd	RuH (1 H)	82.2	$^2J(\text{HP}_M)$	1895 s	2360 s, b ($\nu(\text{B-H}_i)$) 2270 m ($\nu(\text{B-H}_i)$) 1980 m, b ($\nu(\text{B-H}_b)$) 1052 s ($\delta(\text{B-H})$)				
						25.5	$^2J(\text{HP}_Q)$						
						19.2	$^2J(\text{HP}_A)$						
		168	-1.44	b	BH_4 (4 H)								
			1.35	b	BH_4 (3 H)								
			-10.28	b	BH_4 (1 H)								
3	CD_2Cl_2	293	-7.95	dtd	RuH (1 H)	94.3	$^2J(\text{HP}_M)$	1855 s					
						25.7	$^2J(\text{HP}_Q)$						
						21.2	$^2J(\text{HP}_A)$						
4	C_7D_8	333	-6.62	dq	$\text{Ru}(\text{H})_2$ (2 H)	31.1	$^2J(\text{HP}_A)$	1864 s 1722 s					
						6.6	$^2J(\text{HP}_M)$						
						≈ 79	$^2J(\text{HP}_{\text{trans}})$						
						≈ 72	$^2J(\text{HP}_{\text{trans}})$						
6	CD_3COCD_3 ^e	325	-5.34	b	$\text{RuH}(\text{H}_2)$ (3 H)			1930 m					
						223	b			$\text{Ru}(\text{H}_2)$ (2 H)			
							b			$\text{Ru}(\text{H})$ (1 H)			
							dq						
		293	-7.79	dtd	Ru(H) (1 H)	63.3	$^2J(\text{HP}_M)$	1855 s					
				22.5	$^2J(\text{HP}_Q)$								
				22.5	$^2J(\text{HP}_A)$								
8	CD_3COCD_3	293	-7.79	dtd	Ru(H) (1 H)	87.8	$^2J(\text{HP}_M)$	1913 s	2182 s ($\nu(\text{N}\equiv\text{N})$)				
						25.3	$^2J(\text{HP}_Q)$						
						20.6	$^2J(\text{HP}_A)$						
9	CD_3COCD_3	293	-9.02	dq	Ru(H) (1 H)	66.8	$^2J(\text{HP}_M)$	1964 s	1982 s ($\nu(\text{C}\equiv\text{O})$)				
						22.3	$^2J(\text{HP}_Q)$						
						22.3	$^2J(\text{HP}_A)$						
10	CD_3NO_2	293	-7.03	ddt	Ru(H) (1 H)	54.0	$^2J(\text{HP}_M)$	1938 m	1280 s ($\nu(\text{SO})_{\text{asym}}$) 1110 s ($\nu(\text{SO})_{\text{sym}}$) 1100 sh ($\nu(\text{SO})_{\text{sym}}$) 565 s ($\delta(\text{SO}_2)$)				
						19.1	$^2J(\text{HP}_Q)$						
						28.4	$^2J(\text{HP}_A)$						
11	CD_2Cl_2	293	-8.62	dq	Ru(H) (1 H)	80.9	$^2J(\text{HP}_M)$	1920 m, b					
						23.0	$^2J(\text{HP}_Q)$						
						23.0	$^2J(\text{HP}_A)$						
12	CD_2Cl_2	293	2.20	q	NCMe (3 H)	1.5	$^3J(\text{HP})$	2000 m	1035 m (PEt_3 rock)				
						-10.23	dtdd			Ru(H) (1 H)	69.7	$^2J(\text{HP}_M)$	
												19.6	$^2J(\text{HP}_Q)$
												24.2	$^2J(\text{HP}_A)$
				16.7	$^2J(\text{HP}_{\text{PEt}_3})$								
				1.80	m	CH_2 (PEt_3) (6 H)	7.6			$^2J(\text{HP}_{\text{PEt}_3})$			
							1.1			$^4J(\text{HP}_A)$			
							7.5			$^3J(\text{HH})$			
	0.76	dt	CH_3 (PEt_3) (9 H)	13.4	$^2J(\text{HP}_{\text{PEt}_3})$								

^aThe resonances due to the hydrogen atoms of the PP_3 ligand are not reported. ^bKey: d, doublet; t, triplet; q, quartet; m, multiplet; p, pseudo; b, broad. ^c P_A denotes the bridgehead phosphorus atom of the PP_3 ligand, whereas P_M and P_Q indicate the terminal donors of the same ligand. ^dKey: s, strong; m, medium; w, weak; sh, shoulder; b, broad; v, very. ^eThe spectrum was recorded under H_2 .

hydrogen-boron stretch ($\nu(\text{B-H}_i)$), while a broad band centered at 1980 cm^{-1} is assigned to the stretching of the bridging hydrogen-boron bond ($\nu(\text{B-H-Ru})$). The presence of a unidentate BH_4^- ligand is supported by a strong band at 1052 cm^{-1} due to BH_3 deformation. Finally, a sharp, strong absorption at 1895 cm^{-1} shows the compound to contain a terminal hydride ligand.

Treatment of **1** with NaBD_4 in $\text{THF}/\text{C}_2\text{H}_5\text{OD}$ yields the perdeuterated isotopomer [$(\text{PP}_3)\text{Ru}(\text{D})(\eta^1\text{-BD}_4)$] ($2\text{-}d_5$), which exhibits $\nu(\text{B-D}_i)$ at 1778 and 1749 cm^{-1} ($k_{\text{H/D}} = 1.33$ and 1.29 , respectively) and $\nu(\text{B-D}_b)$ at 1646 cm^{-1} ($k_{\text{H/D}} = 1.21$). In addition, a strong absorption at 1376 cm^{-1} is assigned to the stretching of the Ru-D bond ($k_{\text{H/D}} = 1.37$).

The $^31\text{P}\{^1\text{H}\}$ NMR spectrum in CD_2Cl_2 exhibits the expected AMQ_2 splitting pattern (OCT geometry) in the temperature range $+30$ to -100°C . This pattern is maintained in benzene- d_6 , where no line width broadening is observed even at $+75^\circ\text{C}$. The spectrum is temperature-invariant down to -100°C . The ^1H NMR spectrum (CD_2Cl_2 , 20°C) contains a high-field multiplet at -8.52 ppm and a broad hump centered at -1.44 ppm ($w_{1/2} = 141 \text{ Hz}$). The higher field resonance, which appears as a doublet of triplets of doublets, is assigned to the terminal hydride ligand bonded to ruthenium. The dtd multiplicity originates from strong coupling of the hydride to a trans phosphorus atom [$J(\text{HP}_{\text{trans}}) = 82.2 \text{ Hz}$] and to three cis phosphorus nuclei, two of which are magnetically equivalent (Figure 1).

Proton-coupled ^31P NMR spectra unequivocally show the hydride ligand to lie trans to the terminal phosphorus atom P_M . Accordingly, the bridgehead phosphorus atom, P_A , is located trans

to the tetrahydroborate ligand in the fourth equatorial position of the octahedron (II).

The broad resonance at -1.44 ppm in the ^1H NMR spectrum of **2** is assigned to the four hydrogen atoms of the tetrahydroborate ligand. The broadness of this signal is due not only to the quadrupolar interaction with the ^{11}B nucleus but also to a scrambling process, which, at room temperature, makes equivalent the BH_4^- hydrogens. The dynamic process is clearly shown by recording variable-temperature ^1H NMR spectra (benzene- d_6 , temperature range $+75$ to $+5^\circ\text{C}$; CD_2Cl_2 , temperature range $+30$ to -105°C). Like the $^31\text{P}\{^1\text{H}\}$ NMR spectra, the proton spectra are consistent with a fluxional process involving exchange of the BH_4^- hydrogens only. In fact, both the line width and the multiplicity of the high-field signal due to the terminal hydride ligand are temperature-invariant from $+75$ to -105°C . In contrast, the resonance of the four BH_4^- protons broadens as the temperature decreases and, finally, collapses into the baseline at ca. -70°C . Decoalescence of the resonance occurs at -100°C . As a result, two well-separated humps with a 3:1 intensity ratio emerge that exhibit δ values corresponding to the weighted average of the unique fast-exchange resonance observed at room temperature. The lower field and more intense signal centered at ca. 1.35 ppm is partially superimposed on the resonances of the aliphatic chains of the PP_3 ligand. Nevertheless, this resonance can be readily attributed to the three terminal hydrogens of the BH_4^- ligand, whose scrambling process with the bridging hydrogen is largely slowed at the lowest temperature. The other signal ($\delta = -10.28$ ppm), which is more shielded than the hydride ligand

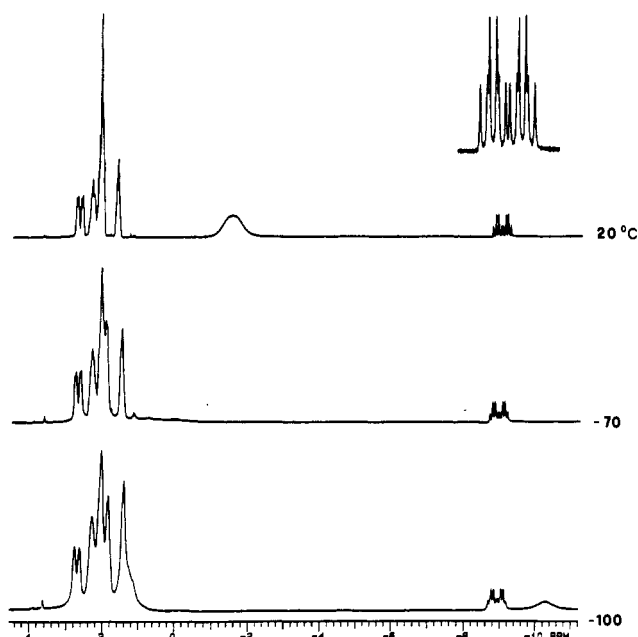


Figure 1. Variable-temperature ^1H NMR spectra of $[(\text{PP}_3)\text{Ru}(\text{H})(\eta^1\text{-BH}_4)]$ in the region +4 to -11 ppm (CD_2Cl_2 , 299.94 MHz, TMS reference).

itself, is readily assigned to the Ru–H–B hydrogen.

The chemistry of **2** is surprisingly rich. The complex decomposes in refluxing toluene or benzene to give the dihydride $[(\text{P}_3)\text{Ru}(\text{H})_2]$ (**4**) (see below) and, presumably, B_2H_6 . Also, **2** exhibits an amphoteric nature, as it reacts with both bases and acids. Stirring **2** in THF with a 2-fold excess of either KO^tBu or PEt_3 for 12 h gives the dihydride **4** and base- BH_3 . Finally, by treatment of **2** in THF with a strong protic acid such as $\text{HOS-O}_2\text{CF}_3$, followed by NaBPh_4 addition, the *cis*-hydride-dihydrogen complex $[(\text{PP}_3)\text{Ru}(\text{H})(\eta^2\text{-H}_2)]\text{BPh}_4$ (**6b**) is quantitatively obtained together with $\text{THF}\cdot\text{BH}_3$ (see below).

Reaction of 1 with LiHBET_3 . Synthesis of $[(\text{PP}_3)\text{Ru}(\text{H})\text{Cl}]$ (3**).** When **1** in THF at room temperature is reacted with a stoichiometric amount of LiHBET_3 (1.0 M in THF) an immediate reaction takes place to give pale yellow crystals of the *cis*-hydride-chloride complex $[(\text{PP}_3)\text{Ru}(\text{H})\text{Cl}]$ (**3**). Selective formation of **3** is obtained also by using a large excess of "superhydride".

In good accord with the results of the reaction of **1** with NaBH_4 , treatment of **3** in THF with a stoichiometric amount of NaBH_4 yields the hydride-borohydride complex **2**.

Complex **3** shares several chemical-physical properties with the parent dichloride **1**. In particular, **3** exhibits a first-order $^{31}\text{P}\{^1\text{H}\}$ NMR AMQ_2 spin system (CD_2Cl_2 , 20 °C), pointing to an OCT structure where the hydride ligand is located trans to the terminal phosphorus and *cis* to chloride, as shown by broadband proton-coupled ^{31}P NMR spectra. A medium-intensity absorbance at 1855 cm^{-1} in the IR spectrum is assigned to $\nu(\text{Ru-H})$. The presence of a terminal hydride ligand is confirmed by the ^1H NMR spectrum, which contains a well-resolved multiplet (dd pattern) at -7.95 ppm (see Table II). This signal can be computed as the X part of an AMQ_2X spin system with a large coupling between the hydride and the trans P atom [$J(\text{HP}_M) = 94.3\text{ Hz}$].

Reaction of 1 with LiAlH_4 . Synthesis of $[(\text{PP}_3)\text{Ru}(\text{H})_2]$ (4**).** The dichloride **1** is quantitatively converted to ivory-colored crystals of the *cis*-dihydride complex $[(\text{PP}_3)\text{Ru}(\text{H})_2]$ (**4**) by treatment with a large excess (ca. 10 equiv) of LiAlH_4 in refluxing THF for 6 h. Decreasing either the amount of LiAlH_4 or the reaction time leads to the formation of mixtures of **4** and of the *cis*-hydride-chloride complex **3**. As anticipated, **4** can be prepared also by thermal decomposition of **2** in refluxing benzene or toluene. The thermal reactions can be conveniently monitored by $^{31}\text{P}\{^1\text{H}\}$ NMR spectroscopy, which shows that the conversion $\mathbf{2} \rightarrow \mathbf{4}$ is

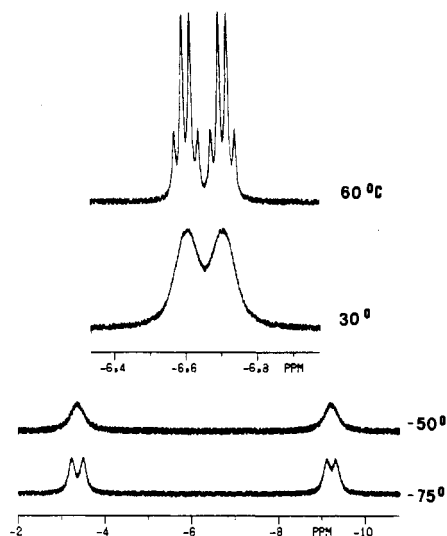


Figure 2. Variable-temperature ^1H NMR spectra of $[(\text{PP}_3)\text{Ru}(\text{H})_2]$ in the hydride region (toluene- d_8 , 299.94 MHz, TMS reference). Intensities have been adjusted to obtain spectra with comparable integral values.

faster in toluene than in benzene.

Complex **4** is air-stable in the solid state for a short time only. It behaves as a nonelectrolyte in deaerated nitroethane and slowly reacts in halogenated hydrocarbons, exchanging chloride for hydride. As an example, **4** in CH_2Cl_2 solution quantitatively transforms into **3** in 3 h. Interestingly, no trace of the dichloride **1** forms within 24 h, thus providing further evidence for the different labilities of the two chloride ligands in **1**.

The IR spectrum of **4** contains two strong $\nu(\text{Ru-H})$ absorptions at 1864 and 1722 cm^{-1} , which are absent in the spectrum of the perdeuterated derivative $[(\text{PP}_3)\text{Ru}(\text{D})_2]$ (**4-d**) [$\nu(\text{Ru-D}) = 1340$ and 1235 cm^{-1} ; $k_{\text{H/D}} = 1.39$] prepared either by deprotonation of $[(\text{PP}_3)\text{Ru}(\text{D})(\text{D}_2)]\text{BPh}_4$ (**6-d**) (see below) with KO^tBu or by reacting **1** with an excess of LiAlD_4 in refluxing THF.

The $^{31}\text{P}\{^1\text{H}\}$ NMR spectrum in toluene- d_8 shows **4** to be fluxional on the NMR time scale. In the fast-exchange limit ($>30\text{ }^\circ\text{C}$), the spectrum consists of an AM_3 spin system and transforms into an AMQ_2 pattern in the slow-exchange limit ($<-75\text{ }^\circ\text{C}$). This dynamic behavior resembles that shown by the iron analogue $[(\text{PP}_3)\text{Fe}(\text{H})_2]^2$ (**5**) with the difference that the slow-exchange regime for ruthenium is attained at a higher temperature (-60 instead of $-80\text{ }^\circ\text{C}$). At $-60\text{ }^\circ\text{C}$, the high-field M_3 portion of the spectrum collapses into a broad hump and then coalesces (ca. $-70\text{ }^\circ\text{C}$). When the sample is further cooled ($-80\text{ }^\circ\text{C}$), decoalescence of this signal takes place to give two resonances (2:1 intensity ratio) which do not resolve into fine structures even at $-100\text{ }^\circ\text{C}$.

The ^1H NMR spectrum of **4** in toluene- d_8 at $60\text{ }^\circ\text{C}$ shows a single doublet of quartets at $\delta = -6.62\text{ ppm}$ for the two hydride ligands (Figure 2). This pattern is due to coupling of instantaneously equivalent hydride ligands to the trans bridgehead phosphorus atom [$J(\text{HP}_{\text{trans}}) = 31.1\text{ Hz}$] and to three equivalent terminal phosphorus atoms of the tripodal polyphosphine [$J(\text{HP}_{\text{cis}}) = 6.6\text{ Hz}$]. Upon a decrease in temperature, the dq pattern at -6.62 ppm broadens and at $30\text{ }^\circ\text{C}$ a signal with no discernible $J(\text{HP})$ coupling constants is observed, thus indicating that the fluxional process is being frozen out. Indeed, this resonance coalesces at $-13\text{ }^\circ\text{C}$ and then emerges at $-50\text{ }^\circ\text{C}$ from the baseline as two broad bumps of equal intensity. Finally, at $-75\text{ }^\circ\text{C}$, each bump resolves into a broad doublet [$\delta = -3.36$, $J(\text{HP}_{\text{trans}}) \approx 79\text{ Hz}$ and $\delta = -9.20\text{ ppm}$, $J(\text{HP}_{\text{trans}}) \approx 72\text{ Hz}$, respectively]. When the sample is heated to $60\text{ }^\circ\text{C}$, the starting multiplet is restored, thus showing the complete reversibility of the dynamic process.

The ^{31}P and ^1H NMR spectra of **4** resemble those of the iron(II) analogue **5**, for which the classical *cis*-dihydride structure was established by the values of T_1 and $J(\text{HD})$.⁵ Indeed, T_1 mea-

(5) Bianchini, C.; Laschi, F.; Peruzzini, M.; Ottaviani, M. F.; Vacca, A.; Zanello, P. *Inorg. Chem.* 1990, 9, 3894.

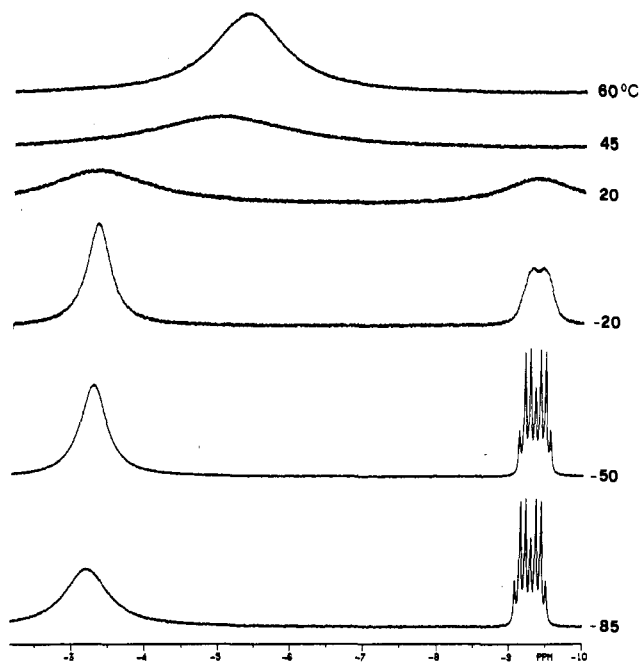


Figure 3. Variable-temperature ^1H NMR spectra of $[(\text{PP}_3)\text{Ru}(\text{H})(\eta^2\text{-H}_2)]\text{PF}_6$ in the hydride region (acetone- d_6 , 299.94 MHz, TMS reference). Intensities have been adjusted to obtain spectra with comparable integral values.

measurements carried out at 300 MHz in toluene- d_8 solutions with the inversion-recovery method gave a spin-lattice relaxation time for **4** of 335 ± 10 ms at 22 °C. This value is largely over the upper limit, which has been considered critical for the presence of a molecular hydrogen ligand.⁶ In particular, genuine ruthenium dihydrogen complexes show T_1 values smaller than that found for **4** by at least 1 order of magnitude.⁷ On the basis of all these data and considerations, a structure can be assigned to **4** where ruthenium is octahedrally coordinated by the four phosphorus donors of PP_3 and by two mutually cis hydrides. The latter ligands exchange very rapidly at room temperature so as to make the three terminal phosphorus atoms of PP_3 equivalent on the NMR time scale, as is the case for trigonal-bipyramidal (TBP) complexes (III).

Synthesis and Characterization of the Molecular Hydrogen Complex $[(\text{PP}_3)\text{Ru}(\text{H})(\eta^2\text{-H}_2)]\text{Y}$ ($\text{Y} = \text{PF}_6$, **6a; BPh_4 , **6b**).** The chemistry of **4** is fully consistent with the classical *cis*-dihydride structure. The compound is not deprotonated by bases whereas it reacts in THF under argon with protic acids such as HOSO_2CF_3 or $\text{HBF}_4 \cdot \text{OEt}_2$ to give off-white crystals of the molecular hydrogen complex $[(\text{PP}_3)\text{Ru}(\text{H})(\eta^2\text{-H}_2)]\text{PF}_6 \cdot \text{C}_2\text{H}_5\text{OH}$ (**6a**) after addition of NH_4PF_6 in ethanol. Substituting NaBPh_4 for NH_4PF_6 gives the unsolvated tetraphenylborate salt **6b**. After taking account of the presence of different counteranions, one sees that complexes **6a** and **6b** exhibit the same chemical-physical properties. Both compounds are moderately stable in the solid state and in solutions of halocarbons, THF, and nitroethane, where they behave as 1:1 electrolytes under an argon atmosphere. Slow decomposition in

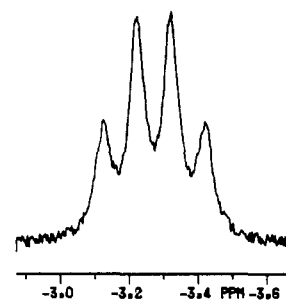


Figure 4. ^1H NMR resonance for the HD proton of the complex cation $[(\text{PP}_3)\text{Ru}(\text{H})(\eta^2\text{-HD})]^+$ (acetone- d_6 , -60 °C, 299.94 MHz, TMS reference).

solution occurs unless a protective H_2 atmosphere is used. Solvents containing the ketone functional group should be avoided because they may react, although slowly, with **6** to give insertion products.⁸ Similarly, coordinating solvents such as DMSO or CH_3CN must be avoided, as they displace the H_2 ligand to form OCT monohydrido adducts (vide infra).

Inspection of IR spectra of **6a,b** does not reveal any absorbance ascribable to $\nu(\text{H-H})$ and $\nu(\text{M-H}_2)$ vibrational modes. Actually, these absorptions are known to be very weak⁹ and, in our case, could be obscured by more intense stretching vibrations such as those of the C-C and C-H bonds of the PP_3 ligand. Besides the typical bands for the PF_6 and BPh_4 counteranions, the only informative IR absorptions are medium-intensity bands at 1930 cm^{-1} (**6a**) and 1955 cm^{-1} (**6b**) due to the terminal Ru-H stretch.

Complex **6a** exchanges the H_2 ligand with D_2 (1 atm) in THF solution to give pure samples of the perdeuterated isotopomer $[(\text{PP}_3)\text{Ru}(\text{D})(\eta^2\text{-D}_2)]\text{PF}_6 \cdot \text{C}_2\text{H}_5\text{OD}$ (**6-d**). Upon deuteration, the $\nu(\text{Ru-H})$ absorption disappears while a new strong absorption appears at 1333 cm^{-1} , which is attributed to $\nu(\text{Ru-D})$ [$k_{\text{H/D}} = 1.45$]. Again, no band due to $\nu(\text{D-D})$ or $\nu(\text{Ru-D}_2)$ modes can be observed.

The variable-temperature ^1H and $^{31}\text{P}\{^1\text{H}\}$ NMR spectra of **6a** in acetone- d_6 are reported in Figures 3 and 5, respectively.

The ^1H NMR spectrum recorded at 52 °C contains a unique broad resonance in the high-field region ($\delta = -5.34$ ppm; $w_{1/2} = 198$ Hz). This signal is typical for hydride- η^2 -dihydrogen complexes where the hydrogens rapidly exchange at the metal center.^{7,10} At 30 °C, this resonance coalesces, and at lower temperature, it emerges from the baseline to give two well-separated bands that at -50 °C fall at -3.29 (2 H) and -9.35 ppm (1 H), respectively. The more intense signal can be readily assigned to the dihydrogen ligand, whose resonance sharpens but does not resolve into fine structure on going from 0 °C ($w_{1/2} = 72$ Hz) to -20 °C ($w_{1/2} = 58$ Hz). Below the latter temperature, the $\eta^2\text{-H}_2$ resonance significantly broadens until at -85 °C a $w_{1/2}$ value of 110 Hz is found.

The resonance at -9.35 ppm, which is therefore assigned to the terminal hydride ligand, resolves into a doublet of quartets at ca. -40 °C. The doublet multiplicity is certainly due to coupling of the hydride ligand to a trans phosphorus atom [$J(\text{HP}_{\text{trans}}) = 63.3$ Hz]. The remaining phosphorus atoms of PP_3 , although non-equivalent (see below), exhibit fortuitous coincidence of their J

(6) (a) Hamilton, D. G.; Crabtree, R. H. *J. Am. Chem. Soc.* **1988**, *110*, 4126. (b) Crabtree, R. H.; Hamilton, D. G. *Adv. Organomet. Chem.* **1988**, *28*, 299.

(7) (a) Chinn, M. S.; Heinekey, D. M. *J. Am. Chem. Soc.* **1987**, *109*, 5865. (b) Conroy-Lewis, F. M.; Simpson, S. J. *J. Chem. Soc., Chem. Commun.* **1987**, 1675. (c) Hampton, C.; Cullen, W. R.; James, B. R.; Charland, J. P. *J. Am. Chem. Soc.* **1988**, *110*, 6918. (d) Hampton, C.; Dekleva, T. W.; James, B. R.; Cullen, W. R. *Inorg. Chim. Acta* **1988**, *145*, 165. (e) Arliguie, T.; Chaudret, B.; Morris, R. H.; Sella, A. *Inorg. Chem.* **1988**, *27*, 598. (f) Arliguie, T.; Chaudret, B. *J. Chem. Soc., Chem. Commun.* **1989**, 155. (g) Joshi, A. M.; James, B. R. *J. Chem. Soc., Chem. Commun.* **1989**, 1785. (h) Jia, G.; Meek, D. W. *J. Am. Chem. Soc.* **1989**, *111*, 757. (i) Amendola, P.; Antonietti, S.; Albertin, G.; Bordignon, E. *Inorg. Chem.* **1990**, *29*, 318. (j) Bautista, M.; Earl, K. A.; Morris, R. H.; Sella, A. *J. Am. Chem. Soc.* **1987**, *109*, 3780. (k) Bautista, M. J.; Earl, K. A.; Maltby, P. A.; Morris, R. H.; Schweitzer, C. T.; Sella, A. *J. Am. Chem. Soc.* **1988**, *110*, 7031.

(8) Work in progress.

(9) (a) Kubas, G. J. *Acc. Chem. Res.* **1988**, *21*, 120. (b) Kubas, G. J.; Unkefer, C. J.; Swanson, B. I.; Fukushima, E. *J. Am. Chem. Soc.* **1986**, *108*, 7000. (c) Eckert, J.; Kubas, G. J.; Hall, J. H.; Hay, P. J.; Boyle, C. M. *J. Am. Chem. Soc.* **1990**, *112*, 2324. (d) Paciello, R. A.; Manriquez, J. M.; Bercaw, J. E. *Organometallics* **1990**, *9*, 260. (10) (a) Crabtree, R. H.; Lavin, M. *J. Chem. Soc., Chem. Commun.* **1985**, 1661. (b) Rhodes, L. F.; Caulton, K. G. *J. Am. Chem. Soc.* **1985**, *107*, 259. (c) Crabtree, R. H.; Lavin, M.; Bonneviot, L. *J. Am. Chem. Soc.* **1986**, *108*, 4032. (d) Lundquist, E. C.; Huffman, J. C.; Foltling, K.; Caulton, K. G. *Angew. Chem., Int. Ed. Engl.* **1988**, *27*, 1165. (e) Bautista, M. T.; Earl, K. A.; Morris, R. H. *Inorg. Chem.* **1988**, *27*, 1124. (f) Bampos, N.; Field, L. D. *Inorg. Chem.* **1990**, *29*, 588. (g) Kim, Y.; Deng, H.; Meek, D. W.; Wojcicki, A. *J. Am. Chem. Soc.* **1990**, *112*, 2798. (h) Luo, X. L.; Crabtree, R. H. *J. Chem. Soc., Chem. Commun.* **1990**, 189. (i) Mediaty, M.; Tachibana, G. N.; Jensen, C. M. *Inorg. Chem.* **1990**, *29*, 3.

values for coupling to the hydride to give a pseudoquartet pattern [$J(\text{HP}_A) \approx J(\text{HP}_Q) \approx 22.5 \text{ Hz}$]. Broad-band proton-coupled ^{31}P NMR spectra at -50°C show the hydride ligand to lie trans to the terminal P_M atom. Accordingly, the molecular hydrogen ligand resides in the equatorial plane of the octahedron trans to the apical P_A atom.

Although the T_1 criterion for recognizing molecular hydrogen complexes has been critically reconsidered,¹¹ we still believe that, at least for simple hydride-dihydrogen species like **6a**, variable-temperature T_1 measurements do provide a useful and reliable criterion for distinguishing classical from nonclassical hydride ligands. Indeed, while the relaxation time for the terminal hydride resonance in **6a** (measured with the inversion-recovery method in acetone- d_6) decreases steadily on raising the temperature from -80°C ($170 \pm 5 \text{ ms}$) to -20°C ($25 \pm 5 \text{ ms}$), the T_1 value for the resonance at -3.29 ppm passes through a flat minimum of $6 \pm 1 \text{ ms}$ over the temperature range -60 to -80°C . This behavior is quite consistent with the presence of a dihydrogen ligand.^{6,11} When the temperature is raised, the T_1 value for the H_2 resonance increases and converges to the value found for the hydride resonance (ca. 20 ms at -13°C). Finally, in the fast-motion regime (52°C), when hydride and dihydrogen are rapidly exchanging at ruthenium, a spin-lattice relaxation time of ca. 25 ms at 52°C is found. T_1 measurements for **6a** in THF- d_8 are similar to those in acetone- d_6 , although the temperature dependence is slightly different [a $T_1(\text{min})$ value of $8 \pm 2 \text{ ms}$ is observed at ca. -40°C].

Intcontrovertible evidence for the hydride- η^2 -dihydrogen structure of **6** is provided by low-temperature ^1H NMR spectra of a ca. 1:1 isotopomeric mixture of $[(\text{PP}_3)\text{Ru}(\text{H})(\text{HD})]^+$ and $[(\text{PP}_3)\text{RuD}(\text{H}_2)]$ (**6-d**) prepared in situ by bubbling deuterium hydride (HD) into an acetone- d_6 solution of the dinitrogen derivative $[(\text{PP}_3)\text{Ru}(\text{H}(\text{N}_2))\text{BPh}_4]$ (**8**) for 5 min. At -60°C , the spectrum exhibits a broad quartet at -3.27 ppm , which is readily assignable to the resonance of the η^2 -coordinated HD molecule (Figure 4). The secondary isotopic shift of 20 ppb exhibited by this signal well matches previously reported data for other η^2 -HD complexes.^{7a,9a,12} The observed multiplicity stems from the 1:1:1 deuterium triplet, which, in turn, splits all of its components into a doublet due to coupling of the H-D proton to the trans bridgehead phosphorus atom of PP_3 . The $J(\text{HD})$ coupling constant of 29.7 Hz confirms the intact nature of the H-D bond. In particular, this value lies in the upper limit for (deuterium hydride)metal complexes (ca. 18 – 34 Hz).^{6b,11a} The strong coupling of HD to the trans phosphorus P_A [$^2J(\text{H}_{\text{HD}}\text{P}_A) \approx ^1J(\text{HD}) = 29.7 \text{ Hz}$] is in line with previous data for other η^2 - H_2 complexes.^{1d,13} Unfortunately, the broadness of this resonance signal (the line width of each component of the quartet is ca. 16 Hz) does not allow one to measure the J values for coupling to the P nuclei that lie cis to the η^2 - H_2 ligand.

Variable-temperature $^{31}\text{P}\{^1\text{H}\}$ NMR spectra of **6a** in acetone- d_6 are shown in Figure 5. At room temperature the spectrum consists of an AM_3 splitting pattern, which is typical for TBP PP_3 complexes, including some cases of η^2 - H_2 derivatives of d^8 metals.^{1d,13} When the temperature is lowered, the fluxional process is frozen out and from -38 to -90°C the spectrum consists of a well-resolved AMQ_2 pattern. The mutual-exchange mechanism that makes equivalent the terminal phosphorus atoms of PP_3 has been studied by DNMR3 spectroscopy assuming exchange between the three configurations $\text{P}_A\text{P}_M\text{P}_Q\text{P}_Q \rightleftharpoons \text{P}_A\text{P}_Q\text{P}_M\text{P}_Q \rightleftharpoons \text{P}_A\text{P}_Q\text{P}_Q\text{P}_M$. A

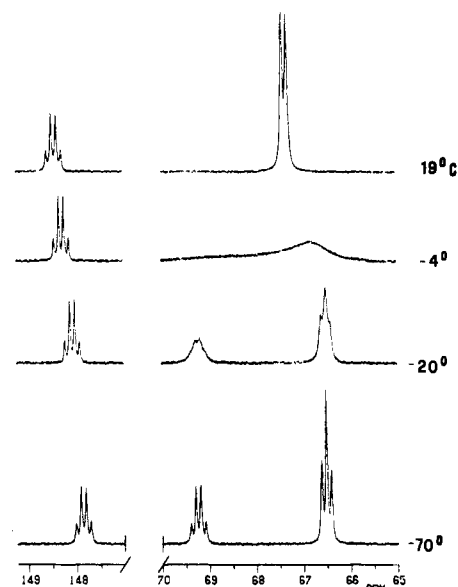


Figure 5. Variable-temperature $^{31}\text{P}\{^1\text{H}\}$ NMR spectra of $[(\text{PP}_3)\text{Ru}(\text{H})(\eta^2\text{-H}_2)]\text{PF}_6$ (acetone- d_6 , 121.42 MHz , $85\% \text{ H}_3\text{PO}_4$ reference).

satisfactory simulation of the variable-temperature spectra has been obtained by using $T_2 = 0.16 \text{ s}$ and the following constants K (s^{-1}): $13\,400$ at 19°C , 7000 at 15°C , 2000 at 5°C , 400 at -4°C , 120 at -10°C , and 20 at -20°C . Plotting $\log K$ against $1/T$ results in a straight line from which the activation parameters ΔH^\ddagger ($24.0 \pm 0.5 \text{ kcal mol}^{-1}$) and ΔS^\ddagger ($44 \pm 3 \text{ cal K}^{-1} \text{ mol}^{-1}$) can be calculated. At the coalescence point, a ΔG^\ddagger value of $12 \pm 1 \text{ kcal mol}^{-1}$ is found, which agrees with the value reported for the iron(II) derivative $[(\text{PP}_3)\text{Fe}(\text{H})(\eta^2\text{-H}_2)]\text{BPh}_4$ (**7**).^{12a} The calculated ΔH^\ddagger and ΔS^\ddagger values are significantly higher than those previously reported for other hydrido(η^2 -dihydrogen)metal complexes.^{10e} However, no value for compounds exhibiting a cis arrangement of H and H_2 has yet been reported. The high E_a value ($24.6 \pm 0.5 \text{ kcal mol}^{-1}$) is consistent with the narrow temperature range for which a variation in the line shape is observed.

Dihydrogen Displacement Reactions. Like the iron(II) analogue $[(\text{PP}_3)\text{Fe}(\eta^2\text{-H}_2)]\text{BPh}_4$ (**7**), complexes **6a,b** are quite robust in the solid state.^{12a} They do not eliminate H_2 even when heated under vacuum (0.1 Torr) for 5 h at 95°C . This spectacular stability is undoubtedly unusual for molecular hydrogen complexes, which normally evolve H_2 at relatively low temperatures and atmospheric pressure.^{6b,11a,14} As an example, the related complex $[\text{Ru}(\text{H})(\eta^2\text{-H}_2)(\text{dppe})_2]\text{BF}_4$ ($\text{dppe} = \text{Ph}_2\text{PCH}_2\text{CH}_2\text{PPh}_2$) loses H_2 at room temperature.¹⁵ In contrast, the H_2 ligand in **6a,b** is rather labile in solution and can be readily displaced at room temperature by a plethora of nucleophiles, including CO , SO_2 , PET_3 , CH_3CN and N_2 . Except for N_2 , these displacement reactions are irreversible; i.e., in no case is the starting η^2 - H_2 complex regenerated by reaction with H_2 .¹⁶

All of the novel complexes are colorless to yellow, crystalline solids that can be isolated as tetraphenylborate salts of formula $[(\text{PP}_3)\text{Ru}(\text{H})(\text{L})]\text{BP}_4$ [$\text{L} = \text{N}_2$ (**8**), CO (**9**), SO_2 (**10**), CH_3CN (**11**), PET_3 (**12**)]. Their IR spectra contain weak to medium

- (11) (a) Crabtree, R. H. *Acc. Chem. Res.* **1990**, *23*, 95. (b) Luo, X. L.; Crabtree, R. H. *Inorg. Chem.* **1989**, *28*, 3777. (c) Ammann, C.; Ischia, F.; Pregosin, P. S. *Magn. Reson. Chem.* **1988**, *26*, 236. (d) Cotton, F. A.; Luck, R. L. *Inorg. Chem.* **1989**, *28*, 2181. (e) Cotton, F. A.; Luck, R. L. *Inorg. Chem.* **1990**, *29*, 43. (f) Luo, X.-L.; Crabtree, R. H. *J. Am. Chem. Soc.* **1990**, *112*, 4813.
- (12) (a) Bianchini, C.; Peruzzini, M.; Zanobini, F. *J. Organomet. Chem.* **1988**, *354*, C19. (b) Conroy-Lewis, F. M.; Simpson, S. J. *J. Chem. Soc., Chem. Commun.* **1986**, 506. (c) Bautista, M. T.; Earl, K. A.; Morris, R. H.; Sella, A. *J. Am. Chem. Soc.* **1987**, *109*, 3780. (d) Chinn, M. S.; Heinekey, D. M. *J. Am. Chem. Soc.* **1990**, *112*, 5166.
- (13) Bianchini, C.; Mealli, C.; Peruzzini, M.; Zanobini, F. *J. Am. Chem. Soc.* **1987**, *109*, 5548.

- (14) Henderson, R. A. *Transition Met. Chem. (London)* **1988**, *13*, 474.
- (15) Morris, R. H.; Sawyer, J. F.; Shiralian, M.; Zubkowsky, J. D. *J. Am. Chem. Soc.* **1985**, *107*, 5581.

- (16) Numerous examples of displacement reactions of η^2 - H_2 ligand are reported in refs 7–15. Other, more specific references: (a) Baker, M. V.; Field, L. D. *J. Organomet. Chem.* **1988**, *354*, 351. (b) Marinelli, G.; Rachidi, I. E. I.; Streib, E.; Eisenstein, O.; Caulton, K. *J. Am. Chem. Soc.* **1989**, *111*, 2346. (c) Albertin, G.; Antonietti, S.; Bordignon, E. *J. Am. Chem. Soc.* **1989**, *111*, 2072. (d) Conroy-Lewis, F. M.; Redhouse, A. D.; Simpson, S. J. *J. Organomet. Chem.* **1989**, *366*, 357. (e) Andriollo, A.; Esteruelas, M. A.; Meyer, U.; Oro, L. A.; Sánchez-Deigado, R. A.; Sola, E.; Valero, C.; Werner, H. *J. Am. Chem. Soc.* **1989**, *111*, 7431. (f) Lundquist, E. C.; Folting, K.; Streib, W. E.; Huffman, J. C.; Eisenstein, O.; Caulton, K. *J. Am. Chem. Soc.* **1990**, *112*, 855. (g) Boyd, S. E.; Field, L. D.; Hambley, T. W.; Young, D. *J. Inorg. Chem.* **1990**, *29*, 1496.

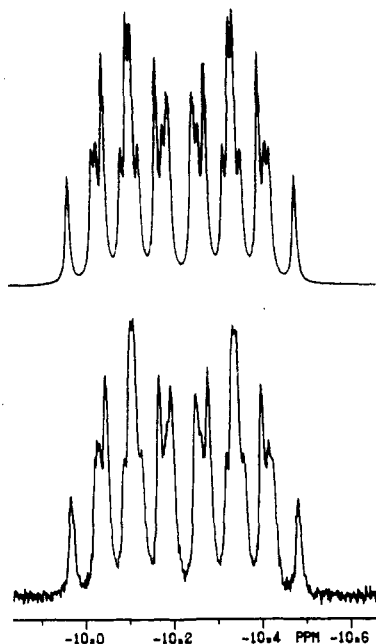


Figure 6. Experimental (lower) and computed (upper) ^1H NMR resonances of the hydride ligand in $[(\text{PP}_3)\text{Ru}(\text{H})(\text{PEt}_3)]\text{BPh}_4$ (CD_2Cl_2 , 20 $^\circ\text{C}$, 299.94 MHz, TMS reference).

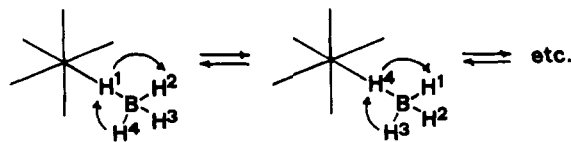
$\nu(\text{Ru}-\text{H})$ bands in the 2000–1913- cm^{-1} region. Obviously, each IR spectrum exhibits characteristic absorbances for the ligand that has replaced H_2 . A list of these IR absorptions is reported in Table II together with $\nu(\text{Ru}-\text{H})$.

Of particular interest is $\nu(\text{N}\equiv\text{N})$ in **8**, which is found at a surprisingly high wavenumber (2182 cm^{-1}) for a dinitrogen ligand that can be easily displaced by dihydrogen. Accordingly, it may be appropriate to enlarge the boundaries of the $\nu(\text{N}\equiv\text{N})$ region (2060–2150 cm^{-1}) where the displacement of the N_2 ligand by H_2 is expected to occur.¹⁷

Compounds **8**–**12** invariably adopt the OCT structure. The $^{31}\text{P}\{^1\text{H}\}$ NMR spectra consist of first-order, temperature-invariant AMQ_2 splitting patterns, except for the spectrum of **12**, which exhibits an AMQ_2V spin system. The resonance of the monophosphine ligand is significantly shifted to high field ($\delta = 6.05$ ppm) as compared to the signals of the phosphorus nuclei of PP_3 . A strong coupling interaction of 211.5 Hz between PEt_3 and the apical phosphorus P_A confirms that the hydride ligand lies trans to the terminal phosphorus P_M .¹⁸ The resonance signal due to the hydride ligand is shown at -10.23 ppm and is rather complicated, as shown in Figure 6. The complex multiplet of the hydride has been computed as the X part of an AMQ_2VX spin (Table II). In all cases the ^1H NMR spectra each exhibit a well-resolved doublet of multiplets for the hydride ligand (-7.03 ppm $\leq \delta \leq -10.23$ ppm) that ^{31}P NMR experiments show to reside trans to P_M in the equatorial plane (II). The multiplicity observed for the hydride ligands arises from strong coupling to the trans phosphorus atom P_M [$54 \text{ Hz} \leq J(\text{HP}_M) \leq 94 \text{ Hz}$] and to three cis phosphorus atoms (P_A and P_Q). The ^1H NMR spectrum of **11** contains a pseudoquartet at 2.20 ppm due to the methyl protons of the coordinated CH_3CN group [$^3J(\text{HP}_M) = ^5J(\text{HP}_Q) = 1.5$ ppm]. No coupling to the terminal phosphorus atom P_A is observed.¹⁹

The sulfur dioxide complex $[(\text{PP}_3)\text{Ru}(\text{H})(\text{SO}_2)]\text{BPh}_4$ (**10**) deserves some additional comment. A planar arrangement of ruthenium and of the S-bonded SO_2 ligand in **10** is supported by the IR spectrum, which contains $\nu(\text{SO})_{\text{asym}}$ and $\nu(\text{SO})_{\text{sym}}$ at 1280

Scheme II



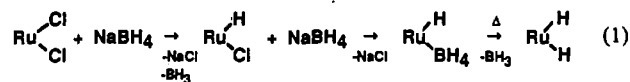
and 1100 cm^{-1} , respectively.²⁰ **10** represents a rare example of a transition-metal complex containing hydride and sulfur dioxide ligands.²¹ This finding is not of trivial importance as one thinks of the increasing interest in the catalytic reduction of SO_2 by metal species. In particular, it has been proposed that complexes containing both hydride and SO_2 ligands would be key intermediates in SO_2 reduction to less polluting products.²²

Discussion

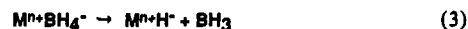
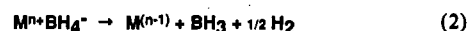
Reactions of $[(\text{PP}_3)\text{RuCl}_2]$ with Main-Group Hydrido Compounds. In the search for a method to replace chlorides with hydrides in **1**, the dichloride was reacted under different conditions with LiAlH_4 , NaBH_4 , and LiHBEt_3 . From our results, it is concluded that the chloride ligands in **1** are not equally metathesized by hydride. One of the chlorides, most likely that trans to the bridgehead phosphorus of PP_3 , offers much more resistance than the other one to being replaced by hydride. As a matter of fact, only LiAlH_4 in drastic reaction conditions proves able to fully exchange hydride for chloride and, therefore, straightforwardly transform **2** into **4**.

Despite possessing nucleophilic properties superior to those of LiAlH_4 or NaBH_4 ,²³ LiHBEt_3 reacts with **1** in THF, selectively yielding the hydride–chloride derivative **3** regardless of the amount of “superhydride”. Raising the temperature to the boiling point does not modify the course of the reaction, likely because of decomposition of LiHBEt_3 before it may react with **3**.

Formation of the dihydride **4** from **1** can be achieved also by using an excess of NaBH_4 in refluxing THF through the three-step sequence schematized in (1).



It is well-known that both thermodynamic and kinetic factors contribute to stabilize covalent metal tetrahydroborate complexes versus either metal reduction as in (2) or hydride formation as in (3).⁴



Indeed, PP_3 appears as appropriately designed for the stabilization of unidentate tetrahydroborate complexes like **2**. In fact, due to its remarkable basicity,^{1,3} this tripodal tetraphosphine is expected to decrease the oxidative tendency of the coordinated metal ions. In addition, the tripodal structure and the six phenyl substituents on the phosphorus donors may play an important kinetic role in stabilizing the tetrahydroborate ligand by saturating and immobilizing the metal coordination sphere (recall that expansion of the metal coordination sphere is required for B–H bond cleavage). In this respect, it is not a case that one of the very few authenticated $\eta^1\text{-BH}_4$ complexes is $[(\text{triphos})\text{CuBH}_4]$ where triphos is the tripodal triphosphine $\text{MeC}(\text{CH}_2\text{PPh}_2)_3$.^{24,25}

- (17) Morris, R. H.; Earl, K. A.; Luck, R. L.; Lazarowich, N. J.; Sella, A. *Inorg. Chem.* **1987**, *26*, 2674.
 (18) Pregosin, P. S.; Kunz, R. W. *^{31}P and ^{13}C NMR of Transition Metal Phosphine Complexes*; Diehl, P., Fluck, E., Kosfeld, R., Eds.; Springer-Verlag: Berlin, 1979.
 (19) Bianchini, C.; Laschi, F.; Ottaviani, M. F.; Peruzzini, M.; Zanello, P.; Zanobini, F. *Organometallics* **1989**, *8*, 893.

(20) Kubas, G. J. *Inorg. Chem.* **1979**, *18*, 183.

(21) Other examples: Levison, J. I.; Robinson, S. D. *J. Chem. Soc., Dalton Trans.* **1972**, 2013. Angoletta, M.; Bellon, P. L.; Manassero, M.; Sansoni, M. *J. Organomet. Chem.* **1974**, *81*, C40. Ryan, R. R.; Kubas, G. J. *Inorg. Chem.* **1978**, *17*, 637.

(22) Kubas, G. J.; Ryan, R. R. *Polyhedron* **1986**, *5*, 473. Kubas, G. J.; Ryan, R. R.; Kubat-Martin, K. A. *J. Am. Chem. Soc.* **1989**, *111*, 7823.

(23) Brown, H. C.; Krishnamurthy, S. *J. Am. Chem. Soc.* **1973**, *95*, 1669.

(24) Ghilardi, C. A.; Midollini, S.; Orlandini, A. *Inorg. Chem.* **1982**, *21*, 4096. Dapporto, P.; Midollini, S.; Sacconi, L. *Inorg. Chem.* **1976**, *15*, 2768.

The tripodal polydentate nature of PP_3 may be responsible also for the unusual dynamic behavior exhibited by **2** in solution. In view of the spectroscopic evidence reported in the previous section, one can readily infer that the fluxionality of **2** is essentially due to the BH_4^- ligand. In particular, neither phosphine arm dissociation nor hydride-tetrahydroborate exchange seems to occur in the equilibration of the BH_4^- hydrogens. A reasonable mechanism through which the tetrahydroborate hydrogens are equilibrated is shown in Scheme II. This involves cleavage of the Ru-H_b-B bridge and interconversion of H_i by rotation. Alternative mechanisms such as the one implying Ru-H_b bond breaking to form the ion pair $[(PP_3)RuH]^+[BH_4]^-$ are ruled out by the results of variable-temperature ^{31}P NMR spectroscopy. Interestingly, **2** and **2-d₃** convert neither into each other nor into other isotopomers by treatment with $D_2O/MeOD$ (or $H_2O/MeOH$) mixtures for 2 h.

A scrambling mechanism like that shown in Scheme II has good precedent for the complex $[RuH(\eta^2-BH_4)(ttp)]$ where ttp is again a polydentate phosphine $[PhP(CH_2CH_2CH_2PPh_2)_2]$.²⁶ As for **2**, neither phosphine nor hydride was found to participate in the fluxional process.

Unlike the fluxionality of **2** that exhibited by the dihydride **4** is evidently of the nonmutual-exchange type, since it involves both phosphorus and hydride ligands (Figure 2). As for the iron(II) analogue **5**,⁵ equilibration of hydride and terminal phosphorus of PP_3 does not require H-H bonding to give an η^2 -dihydrogen derivative.

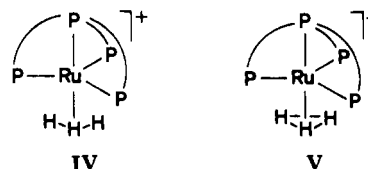
In all of the OCT Ru(II) complexes herein described, the hydride ligand is located trans to the terminal phosphorus P_M of PP_3 (II). No trace of the other possible geometric isomer (i.e. the one containing hydride trans to P_A) is observed by NMR spectroscopy. This stereospecific arrangement is quite typical for OCT metal complexes with PP_3 and is independent of the nature of both the metal and the sixth coligand.³ The most straightforward interpretation of this stereospecificity is to think of electronic effects, particularly the well-known propensity of the hydride ligand to lie trans to the ligand showing the lowest trans influence among those completing the metal coordination sphere. In this respect, it is worth mentioning that, in OCT complexes, the bridgehead phosphorus atom P_A of PP_3 is more tightly bound to the metal than the terminal ones.²⁸

The Dihydrogen Complex $[(PP_3)RuH(\eta^2-H_2)]^+$. From a comparison of the NMR data for **6b** with those previously reported for the isoelectronic and isostructural iron(II) derivative **7**,^{12a} one may readily infer that the two compounds share a fluxionality of the same type, the only difference being that the intramolecular exchange of hydrogens is thermodynamically easier for Fe. At the coalescence point, ΔG^\ddagger values of 12.1 ± 0.3 and 12 ± 1 kcal mol⁻¹ are calculated for **7** and **6b**, respectively.

In the slow-exchange limit, both compounds exhibit temperature dependence of the line width of the H_2 signal; i.e., upon a decrease in temperature the resonance broadens. This effect is quite common for transition-metal dihydrogen complexes and has been ascribed to a changeover of the correlation time of the molecule as a whole on going from the extreme narrowing to the slow-motion regimes.²⁹ In the related OCT complexes $[M(H)(H_2)(dppe)_2]BF_4$ ($M = Fe, Ru$),¹⁵ the broadening of the H_2 signal has been attributed to hindered rotation of the molecule on the square face of a square pyramid defined by the four phosphorus donors and by the terminal hydride (notice that, except for containing a different geometrical arrangement of hydride and

dihydrogen ligands, the PP_3 and dppe complexes are quite comparable). Actually, the broadening of the H_2 resonance may be well due to the well-known decrease in T_2 with a decrease of the temperature (recall that T_2 controls the line width of the resonance: $w_{1/2} = 1/\pi T_2$).⁶

The mechanistic aspect of the major fluxional process exhibited by the Ru and Fe complexes $[(PP_3)M(H)(H_2)]^+$, namely the intramolecular exchange of the hydrogens, is much more difficult to address. The ^{31}P NMR data clearly indicate that in the fast-exchange limit the three hydrogen atoms occupy axial positions trans to the bridgehead phosphorus of PP_3 . In particular, the absence of detected free phosphine arms and the sharpness of the resonances seem to rule out any trihydride intermediate in the exchange mechanism. However, our experimental evidence does not discriminate between the two possible structures through which hydride and dihydrogen are believed to exchange, i.e. the open (IV) or closed (V) H_3 units.³⁰



As a final consideration, we note that the trends in the barriers to intramolecular exchange of the hydrogens, in the susceptibilities to H_2 loss or replacement, in the $\nu(N\equiv N)$ stretching frequencies, in the T_1 values, and in the $J(HD)$ coupling constants are all consistent with an H-H bonding interaction greater for ruthenium than for iron.⁵ Quite similar trends have been previously observed for other hydride-dihydrogen complexes of the iron triad.^{7ij}

Experimental Section

General Data. Tetrahydrofuran, toluene, and dichloromethane were purified by distillation over $LiAlH_4$, sodium, and P_2O_5 under nitrogen just prior to use, respectively. All the other solvents and chemicals were reagent grade and, unless otherwise stated, were used as received by commercial suppliers. Deuterated solvents for NMR measurements were dried over molecular sieves. The ruthenium starting products $[RuCl_2(DMSO)_4]$ ³¹ and $[RuCl_2(PPh_3)_4]$ ³² were prepared according to literature methods. High-purity HD was prepared from D_2O and $LiAlH_4$ according to the procedure described by Wender et al.³³ Infrared spectra of samples milled in Nujol between KBr plates were recorded on a Perkin-Elmer 1600 Series FTIR spectrophotometer. Proton NMR spectra were recorded at 299.945 MHz on a Varian VXR 300 spectrometer. Peak positions are relative to tetramethylsilane as external reference. $^{31}P\{^1H\}$ NMR spectra were recorded on the same instrument operating at 121.42 MHz. Chemical shifts are relative to external 85% H_3PO_4 , with downfield values reported as positive. Conductivities were measured with an ORION Model 990101 conductance cell connected to a Model 101 conductivity meter. The conductivity data were obtained at sample concentrations at ca. 1×10^{-3} M in nitroethane solutions at room temperature (20 °C). The computer simulation of NMR spectra was carried out with a locally developed package containing the programs LAOCN3³⁴ and DAVINS,³⁵ running on a Compaq Deskpro 386/25 personal computer. The initial choices of shifts and coupling constants were refined by iterative least-squares calculations using the experimental digitized spectrum. The final parameters gave a satisfactory fit between experimental and calculated spectra, the agreement factor R being less

(25) Other examples of η^1-BH_4 complexes are reported in: Jensen, J. A.; Girolami, G. S. *J. Am. Chem. Soc.* **1988**, *110*, 445.

(26) Letts, J. C.; Mazanec, T. J.; Meek, D. W. *J. Am. Chem. Soc.* **1982**, *104*, 3898.

(27) Some examples of P_A -metal and P_M -metal bond lengths in OCT PP_3 complexes are as follows: 2.271 (1) vs 2.358 (1) Å in $[(PP_3)RhH_2]^+$,¹³ 2.161 (2) (average) vs 2.211 (2) (average) Å in $[(PP_3)Fe(OOCR)]^+$ ($R = Ph, OC_2H_5$);²⁸ 2.18 (1) vs 2.22 (1) Å in $[(PP_3)Co(H)(C\equiv CSiMe_3)]^+$.²⁸

(28) To be published.

(29) Ricci, J. S.; Koetzle, T. F.; Bautista, M. T.; Hofstede, M. T.; Morris, R. H.; Sawyer, J. F. *J. Am. Chem. Soc.* **1989**, *111*, 8823.

(30) (a) Heinekey, D. M.; Millar, J. M.; Koetzle, T. F.; Payne, N. G.; Zilm, K. W. *J. Am. Chem. Soc.* **1990**, *112*, 909. (b) Zilm, K. W.; Heinekey, D. M.; Millar, J. M.; Payne, N. G.; Neshyba, S. P.; Duchamp, J. C.; Szczyrba, J. *J. Am. Chem. Soc.* **1990**, *112*, 920 and references therein. For a theoretical paper see: Burdett, J. K.; Phillips, J. R.; Pourian, M. R.; Poliakov, M.; Turner, J. J.; Upmacis, R. *Inorg. Chem.* **1987**, *26*, 3054.

(31) Evans, I. P.; Spencer, A.; Wilkinson, G. *J. Chem. Soc., Dalton Trans.* **1973**, 204.

(32) Hallman, P. S.; Stephenson, T. A.; Wilkinson, G. *Inorg. Synth.* **1970**, *12*, 237.

(33) Wender, I.; Friedel, R. A.; Orchin, M. *J. Am. Chem. Soc.* **1949**, *71*, 1140.

(34) Castellano, S.; Bothner-By, A. A. *J. Chem. Phys.* **1964**, *41*, 3863.

(35) Stephenson, D. S.; Binsch, G. *J. Magn. Reson.* **1980**, *37*, 395. Stephenson, D. S.; Binsch, G. *J. Magn. Reson.* **1980**, *37*, 395.

than 1% in all cases. The line-shape analysis of the variable-temperature NMR spectra was accomplished by means of the DNMR3 program³⁶ adapted for the Compaq computer. Errors in the calculated rate constants were estimated by varying the rate constant around the best-fit value, until an observable difference between simulated and experimental spectra, both displayed on the graphical terminal, could be detected. These errors proved to be 10% or less.

Synthesis of the Complexes. All reactions and manipulations were routinely performed under a dry nitrogen atmosphere by using Schlenk-tube techniques. The solid compounds were collected on sintered-glass frits and washed with ethanol and petroleum ether (bp 50–70 °C) before being dried in a stream of nitrogen.

Preparation of [(PP₃)RuCl₂](1). Method A. A 5.00-g (10.32-mmol) sample of [RuCl₂(DMSO)₂] and 7.00 g (10.44 mmol) of PP₃ were dissolved in 200 mL of toluene, and the solution was heated to reflux temperature. The reflux was maintained for 2 h, during which time 1 separated as a yellowish crystalline product. The precipitation of 1 was completed by cooling the mixture down to 0 °C with an ice bath. The crude product (yield 85–90%) was used for the synthesis of all the other PP₃Ru complexes herein described without further purification. Analytically pure product was obtained as the dichloromethane solvate after recrystallization from CH₂Cl₂/EtOH. Anal. Calcd for C₄₃H₄₄Cl₂P₄Ru: C, 55.68; H, 4.78; Cl, 15.29; Ru, 10.90. Found: C, 55.44; H, 4.71; Cl, 15.47; Ru, 10.73.

Method B. A 12.20-g (9.99-mmol) sample of [RuCl₂(PPh₃)₄] and 7.00 g (10.44 mmol) of PP₃ were reacted in toluene (250 mL) in a fashion similar to that described above. The yield of the crude product was ca. 70–75%.

Preparation of [(PP₃)Ru(H)(η¹-BH₄)](2). A solution of NaBH₄ (0.08 g, 2.10 mmol) in hot ethanol (25 mL) was added portionwise during 5 min to a well-stirred solution of 1 (0.85 g, 1.01 mmol) in THF (60 mL) maintained at 50 °C. Immediately the solution turned colorless. Addition of ethanol (50 mL) to the reaction mixture cooled to room temperature and slow evaporation of the solvent yielded pale cream-colored crystals of 2. Yield: 80%. Anal. Calcd for C₄₂H₄₇BP₄Ru: C, 64.05; H, 6.02; Ru, 12.83. Found: C, 63.87; H, 6.00; Ru, 12.76.

The perdeuterated derivative [(PP₃)RuD(η²-BD₄)](2-d₃) was prepared in the same way by using NaBD₄ and C₂H₅OD.

Preparation of [(PP₃)Ru(H)Cl](3). Method A. Neat LiHBEt₃ (1.25 mL of a 1.0 M THF solution, 1.25 mmol) was syringed into a THF (50 mL) solution of 1 (1.00 g, 1.19 mmol) to produce a clear yellow solution that deposited pale yellow crystals of 3 after addition of ethanol (60 mL). Yield: 90%. Anal. Calcd for C₄₂H₄₃ClP₄Ru: C, 62.42; H, 5.36; Cl, 4.39; Ru, 12.51. Found: C, 62.30; H, 5.48; Cl, 4.28; Ru, 12.36.

Method B. A solution of NaBH₄ (0.04 g, 1.06 mmol) in hot ethanol (10 mL) was added portionwise to a solution of 1 (0.85 g, 1.01 mmol) in THF (25 mL). Addition of ethanol (15 mL) gave 3. Yield: 95%.

Preparation of [(PP₃)Ru(H)₂](4). A 2.50-g (65.88-mmol) quantity of solid LiAlH₄ was added portionwise to a stirred suspension of 5.00 g (5.93 mmol) of 1 in 300 mL of THF. The slurry was gently heated to reflux temperature and stirred for 7 h. Then, the flask was cooled with an ice bath and excess LiAlH₄ was hydrolyzed by careful addition of a mixture of THF/H₂O (50 mL, 3:1 v/v) through a dropping funnel. The slurry was filtered to remove all the lithium and aluminum hydrolysis products, and a clear, occasionally pale yellow, solution was obtained. THF was distilled off until the volume of the solution was reduced to ca. 80 mL. On addition of ethanol (100 mL) and slow concentration of the resulting mixture, ivory-colored crystals of 4 separated. Yield: ca. 80%. Anal. Calcd for C₄₂H₄₄P₄Ru: C, 65.19; H, 5.73; Ru, 13.06. Found: C, 65.02; H, 5.88; Ru, 12.90.

The perdeuterated derivative [(PP₃)RuD₂](4-d₂) was prepared by substituting LiAlD₄ and C₂H₅OD for LiAlH₄ and C₂H₅OH in the above procedure.

Thermal Decomposition of 2. A solution of 2 (0.50 g, 0.63 mmol) in benzene or toluene (50 mL) was slowly brought to reflux temperature. After 2 h, the solution was cooled with an ice bath and ethanol (60 mL) was added. Complex 4 was obtained in ca. 60% yield.

Preparation of [(PP₃)RuH(η²-H₂)]PF₆·C₂H₅OH (6a). Neat HOSO₂CF₃ (0.18 mL, 2.04 mmol) was syringed into a THF suspension (70 mL) of 4 (1.50 g, 1.94 mmol) under a positive pressure of H₂. The mixture was stirred for 20 min, during which time the starting product dissolved to give a colorless solution. Addition of NH₄PF₆ (0.42 g, 2.58 mmol) and ethanol (100 mL) yielded white crystals of 6a. Yield: 85%. $\Lambda_M = 83 \Omega^{-1} \text{ cm}^2 \text{ mol}^{-1}$. Anal. Calcd for C₄₄H₅₁F₆OP₃Ru: C, 54.72; H, 5.32; Ru, 10.46. Found: C, 54.59; H, 5.35; Ru, 10.40.

Preparation of [(PP₃)RuH(η²-H₂)]BPh₄ (6b). The unsolvated tetraphenylborate salt was prepared in ca. 90% yield by substituting NaBPh₄ (0.85 g, 2.50 mmol) for NH₄PF₆ in the above procedure. $\Lambda_M = 41 \Omega^{-1} \text{ cm}^2 \text{ mol}^{-1}$. Anal. Calcd for C₆₆H₆₃BP₄Ru: C, 72.46; H, 5.99; Ru, 9.24. Found: C, 72.36; H, 6.02; Ru, 9.20.

A ca. 1:1 isotopomeric mixture of [(PP₃)Ru(H)(η²-HD)]BPh₄ and [(PP₃)Ru(D)(η²-H₂)]BPh₄ (6-d₁) was prepared in situ by bubbling gaseous HD for 10 min throughout an acetone-d₆ solution of [(PP₃)-(RuH(N₂))]BPh₄ (8) into an NMR tube cooled at 0 °C.

Preparation of [(PP₃)RuH(N₂)]BPh₄ (8). Method A. Neat CH₃OS- O₂CF₃ (114 μL, 1.00 mmol) was syringed into a THF solution of (50 mL) of 4 (0.75 g, 0.96 mmol) under an atmosphere of dry nitrogen. On addition of NaBPh₄ (0.45 g, 1.32 mmol) and ethanol (70 mL), sand-colored crystals of 8 were obtained in ca. 90% yield.

Method B. The dinitrogen complex 8 was obtained in almost quantitative yield by bubbling N₂ throughout a THF solution of 6b for 30 min, followed by addition of ethanol and concentration of the resulting solution. $\Lambda_M = 39 \Omega^{-1} \text{ cm}^2 \text{ mol}^{-1}$. Anal. Calcd for C₆₆H₆₃BN₂P₄Ru: C, 70.78; H, 5.67; N, 2.50; Ru, 9.02. Found: C, 70.59; H, 5.74; N, 2.15; Ru, 8.88.

Preparation of [(PP₃)RuH(CO)]BPh₄ (9). The hydride-carbonyl complex 9 was prepared by bubbling CO for 5 min throughout a THF solution of 6b or 8. On addition of ethanol and concentration of the solution, white crystals of 9 precipitated. Yield: 90%. $\Lambda_M = 47 \Omega^{-1} \text{ cm}^2 \text{ mol}^{-1}$. Anal. Calcd for C₆₇H₆₃BOP₄Ru: C, 71.85; H, 5.67; Ru, 9.02. Found: C, 71.86; H, 5.64; Ru, 8.79.

Preparation of [(PP₃)RuH(SO₂)]BPh₄ (10). Gaseous SO₂ was passed through a THF solution of 6b or 8 for 5 min. During this time, the solution became orange. After addition of ethanol, yellow crystals of 10 separated. Yield: 70%. $\Lambda_M = 43 \Omega^{-1} \text{ cm}^2 \text{ mol}^{-1}$. Anal. Calcd for C₆₆H₆₃BO₂P₄RuS: C, 68.57; H, 5.49; Ru, 8.74; S, 2.77. Found: C, 68.39; H, 5.37; Ru, 8.60; S, 2.53.

Preparation of [(PP₃)RuH(CH₃CN)]BPh₄ (11). Neat acetonitrile (0.50 mL, 9.55 mmol) was pipetted into a THF solution (20 mL) of 6b or 8 (ca. 0.50 mmol). After 10 min, ethanol (25 mL) was added and the reaction mixture was concentrated until pale yellow crystals of 11 separated. Yield: 85%. $\Lambda_M = 44 \Omega^{-1} \text{ cm}^2 \text{ mol}^{-1}$. Anal. Calcd for C₆₈H₆₆BNP₄Ru: C, 71.89; H, 5.86; N, 1.23; Ru, 8.90. Found: C, 71.78; H, 5.90; N, 1.07; Ru, 8.82.

Preparation of [(PP₃)RuH{P(C₂H₅)₃}]BPh₄ (12). Neat triethylphosphine (0.25 mL, 1.69 mmol) was pipetted into a THF solution (20 mL) of 6b or 8 (ca. 0.50 mmol). After 10 min, ethanol was added. Concentration of the resulting solution under a brisk current of nitrogen yielded sand-colored microcrystals of 12. Yield: 70%. $\Lambda_M = 39 \Omega^{-1} \text{ cm}^2 \text{ mol}^{-1}$. Anal. Calcd for C₇₂H₇₈BNP₃Ru: C, 71.46; H, 6.50; Ru, 8.35. Found: C, 71.42; H, 6.43; Ru, 8.21.

Reaction of 6 with KO^tBu. Solid KO^tBu (0.06 g, 0.53 mmol) was added to a stirred THF solution (20 mL) containing ca. 0.50 mmol of 6a,b under a H₂ atmosphere. After 10 min, dihydrogen was replaced with nitrogen and deareated ethanol (30 mL) was added. After concentration of the solution, ivory-colored crystals of 4 separated in 90% yield. Under similar conditions, a large excess of triethylamine did not deprotonate 6a,b.

Reaction of 2 with HOSO₂CF₃. Neat HOSO₂CF₃ (20 mL, 0.23 mmol) was syringed into a stirred THF (20 mL) suspension of 2 (0.16 g, 0.20 mmol) under dihydrogen. The starting solid immediately dissolved to produce a colorless solution that upon addition of solid NaBPh₄ (0.20 g, 0.60 mmol) and ethanol (30 mL) yielded colorless crystals of 6b. Yield: 90%. When the same reaction was accomplished under a N₂ atmosphere, complex 8 was obtained in ca. 80%.

Acknowledgment. This work was supported by grants from the CNR program "Progetti Finalizzati II, Chimica Fine e Secondaria" and EEC (Brussels) Contract SC1.0027.c.

(36) Kleier, D. A.; Binsch, G. A Computer Program for the Calculation of Complex Exchange-Broadened NMR Spectra, QCPE Program No. 165.